Article

Tailoring the Key in a Molecular Lock-and-Key Model System: The Propylene Oxide···2-Fluoroethanol Complex

Nicole Borho, and Yunjie Xu

J. Am. Chem. Soc., **2008**, 130 (18), 5916-5921 • DOI: 10.1021/ja0783411 • Publication Date (Web): 11 April 2008

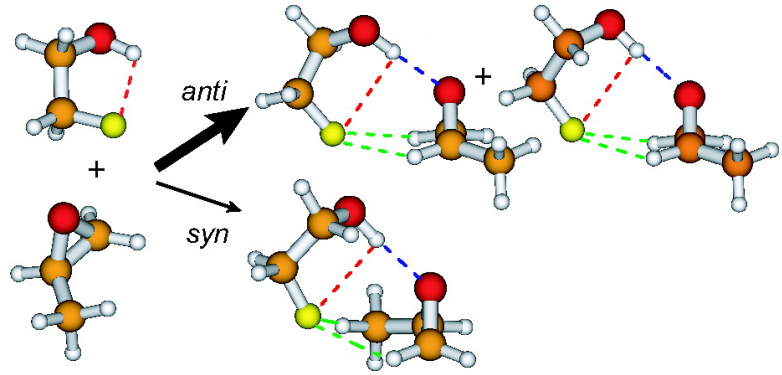

J|A|C|S
ARTICLES

Published on Web 04/11/2008

Tailoring the Key in a Molecular Lock-and-Key Model System: The Propylene Oxide···2-Fluoroethanol Complex

Nicole Borho and Yunjie Xu*

Department of Chemistry, University of Alberta, Edmonton, Alberta, Canada, T6G 2G2

Received October 31, 2007; E-mail: yunjie.xu@ualberta.ca

Abstract: The conformational isomerism of the propylene oxide (PO)···2-fluoroethanol (FE) complex has been investigated using molecular beam Fourier-transform microwave spectroscopy complemented with high level ab initio calculations. Rotational transitions of three different binary conformers have been observed experimentally. On the basis of the agreement of the experimental and calculated rotational constants, they could be identified as the three most stable structures, *anti G*−*g*+, *anti G*+*g*−, and *syn G*+*g*−. All the observed structures exhibit a primary O−H···O hydrogen bond, an intramolecular O−H···F hydrogen bond and two secondary intermolecular C−H···F contacts. The two *anti* conformers, with FE and the PO methyl group on the opposite sides of the oxirane ring, show higher abundances than the *syn* conformer. In all three observed conformers, FE remains approximately in its favorable compact gauche conformation. The monofluorination of the molecular lock-and-key model system PO···ethanol increases not only the number of possible binary conformers, but also the discrimination energy among them. The superior discrimination ability of FE as compared to ethanol classifies it as a tailored key to the PO lock.

1. Introduction

Biochemical processes in the chemistry of life often exhibit high specificity. This molecular recognition[1] phenomenon was noticed as early as 1894 when Fischer coined his famous lock-and-key principle[2] for the interactions of a substrate-template complex. His metaphor emphasizes on the geometrical compatibility of the two binding partners. In recent decades, structural information about numerous protein–ligand complexes determined via X-ray crystallography and NMR spectroscopy has been documented, for example, in the Cambridge Structural Database[3] and the Protein Data Bank.[4] Analysis of the structural data reveals that flexible ligands often change their monomer conformations dramatically upon complex formation,[5,6] in accord with the induced fit theory proposed by Koshland.[7] Consequently, some researchers deem this situation "rusting of the lock and key model for protein–ligand binding".[8] The ongoing debate about the fundamental concept of molecular recognition highlights the necessity of an accurate description of the intermolecular interactions in substrate−template complexes. Our approach is to start from the analysis of small, isolated model systems with well-defined intermolecular interaction sites and a limited number of flexible bonds. We take advantage of jet-cooled rotational spectroscopy for providing accurate structural information and utilize it to identify different conformers. In addition, we can establish their stability trend on the basis of the observed relative line intensities.

One such model complex is propylene oxide (PO)···ethanol. It was characterized previously[9] and was interpreted as a microscopic example of Fischer's lock-and-key metaphor. There, ethanol acts as a donor in a primary O−H···O hydrogen (H)-bond and offers three shapes of keys in the form of three conformers. The rigid molecule PO acts as a H-bond acceptor and can be viewed as a solid lock. All six possible conformers were observed.[9] This points to small differences in binding energy among them and indicates a limited selectivity of the PO···ethanol interaction. To increase the specificity of the interaction, we decided to fluorinate the H-bond donor ethanol, thus adding another differentiating "tooth" to the key molecule.

Fluorination has a dramatic impact on the molecular properties of an organic molecule. It influences the bioavailability, metabolic stability, and biological activity, and has gained importance in the life science industry in the past decade.[10] An important application of fluoroethanols, most commonly 2,2,2-trifluoroethanol, is their usage as cosolvents for peptides and proteins. Addition of fluoroalcohols to an aqueous protein solution can alter the secondary and tertiary structures of proteins.[11,12] It is proposed that the modification of the protein

(1) Suhm, M. *Phys. Chem. Chem. Phys.* **2007**, *9*, 4443.
(2) Fischer, E. *Chem. Ber.* **1894**, *27*, 2985.
(3) Allen, F. H.; Bellard, S.; Brice, M. D.; Cartwright, B. A.; Doubleday, A.; Higgs, H.; Hummelink, T.; Hummelink-Peters, B. G.; Kennard, O.; Motherwell, W. D. S.; Rodgers, J. R.; Watson, D. G. *Acta Crystallogr.* **1979**, *B35*, 2331–2339.
(4) Bernstein, F. C.; Koetzle, T. F.; Williams, G. J. B., Jr.; Meyer, E. F.; Brice, M. D.; Rogers, J. R.; Kennard, O.; Shimanouchi, T.; Tasumi, M. *J. Mol. Biol.,* **1977**, *112*, 535–542.
(5) Nicklaus, M. C.; Wang, S.; Driscoll, J. S.; Milne, G. W. A. *Bioorg. Med. Chem.* **1995**, *3* (4), 411–428.
(6) Perola, E.; Charifson, P. S. *J. Med. Chem.* **2004**, *47*, 2499–2510.
(7) Koshland, D. E., Jr *Proc. Natl. Acad. Sci., U.S.A.* **1958**, *44*, 98–104.
(8) Jorgensen, W. L. *Science* **1991**, *254*, 954–955.
(9) Borho, N.; Xu, Y. *Angew. Chem.* **2007**, *119,* 2326−2329. *Angew. Chem., Int. Ed.* **2007**, *46*, 2276–2279.
(10) Maienfisch, P.; Hall, R. G. *Chimia* **2004**, *58* (3), 93–99.
(11) Povey, J. F.; Smales, C. M.; Hassard, St. J.; Howard, M. J. *J. Struct. Biol.* **2007**, *157*, 329–338.
(12) (a) Buck, M. Q. *Rev. Biophys.* **1998**, *31* (3), 297–355. (b) Scharge, T.; Cézard, C.; Ziehlke, P.; Schütz, A.; Emmeluth, C.; Suhm, M. A. *Phys. Chem. Chem. Phys.* **2007**, *9*, 4472–4490. (c) Fioroni, M.; Diaz, M. D.; Burger, K.; Berger, S. *J. Am. Chem. Soc.* **2002**, *124*, 7737–7744.

10.1021/ja0783411 CCC: $40.75

folding is caused by intermolecular interactions between the protein and the fluoroalcohol solvent. But the underlying mechanism, for example, the role of H-bonding in comparison to electrostatic interactions is still under discussion.[12] This is yet another motivation to investigate the intermolecular interactions in fluoroalcohols and between fluoroalcohols and solutes.

In our current study, we investigate the interaction of PO and 2-fluoroethanol (FE), extending the original lock-and-key model system by monofluorination. The substitution of a H atom by a F atom has only a minor sterical effect because of their comparable van der Waals radii (1.20 Å vs 1.47 Å for H and F, respectively), but a major effect on the polarity of the substituted molecule since the electronegativities of H and F differ significantly (2.2 vs 4.0 on the Pauling scale).[13] Furthermore, the presence of the fluorine functional group enables intramolecular O−H···F and additional intermolecular C−H···F interactions.[14] The increase in the number of contact points is expected to significantly enhance the discrimination ability[15] of FE in choosing its preferred orientation in the PO···FE complex. By tailoring the key molecule in our microscopic lock-and-key model system, we aim to understand the discrimination mechanism at play and to gain insight into the interactions in the fluoroalcohol solvent-substrate complexes. In this article, we present rotational spectroscopic and *ab initio* studies of the PO···FE interaction pair.

2. Methods

A. Experimental Methods. The rotational spectra were recorded with a Balle−Flygare-type[16] pulsed molecular beam FTMW spectrometer, operated in the frequency region between 3.5 and 16 GHz. The details of the spectrometer were described before.[17] A gas mixture of 0.3% *R*-PO (≥99.0%, Aldrich) and 0.3% FE (97%, Sigma-Aldrich) in 1–5 bar Neon (Ne) (99.9990%) or Helium (He) (99.996%) was expanded through a pinhole nozzle to generate the PO···FE complex. The uncertainty of the frequency measurements is about 1–2 kHz and the full line width at half-height is about 18 kHz in Ne and 22 kHz in He.

B. Computational Methods. The exploration of the conformational landscape of the PO···FE interaction pair was performed in Gaussian 03,[18] using the second-order Møller–Plesset perturbation theory (MP2)[19] with the 6-311++G(d,p) basis set.[20] The true minimum nature of the optimized geometries was indicated by the nonimaginary character of the harmonic frequencies calculated at the respective optimized geometries. The zero-point-energy (ZPE) corrections were obtained from the same calculations. Basis set superposition error (BSSE) corrections were determined using the counterpoise correction methods of Boys and Bernardi.[21]

3. Conformational Isomerism. The binary PO···FE complex can adapt different geometries that are defined by the conformation of the FE subunit and the relative arrangement of FE and PO in the complex. The PO subunit is rigid since its methyl group internal

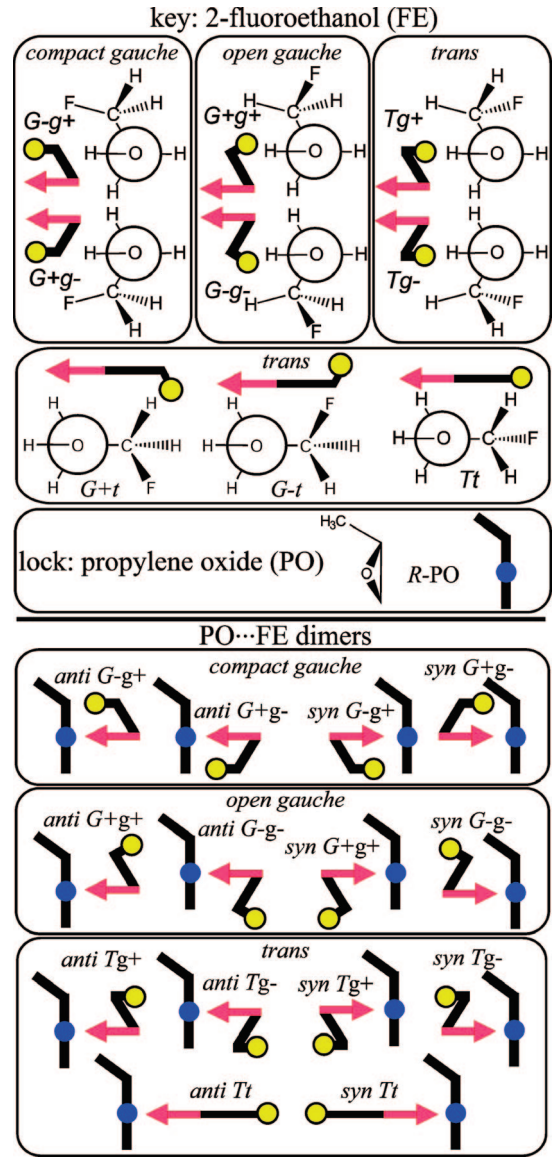

Figure 1. Schematic view of the nine FE monomer conformers, of PO monomer, and of the 14 PO···FE dimer conformers.

rotation motion[22,23] is quenched in the complex.[24] The structure of PO was determined by rotational spectroscopy.[25,26] FE has two structural relevant torsional angles $\tau_{O-C-C-F}$ and $\tau_{H-O-C-C}$. They adapt approximately +60, −60, or 180° and are labeled with gauche+ (*G*+), gauche− (*G*−), and trans (*T*) with capital letters for $\tau_{O-C-C-F}$, and *g*+, *g*−, and *t* with small letters for the $\tau_{H-O-C-C}$ torsional angle, following the notation of ref 27. The additional torsional degree of freedom of FE in comparison to ethanol increases the number of possible conformers from 3 to 9. A schematic view of the nine FE conformers is given in the upper part of Figure 1. They are grouped into compact gauche, open

(13) Pauling, L., *The Nature of the Chemical Bond*, 3rd ed.; Cornell University:, Ithica, NY, 1960.
(14) Desiraju, G. R, Steiner, T., *The Weak Hydrogen Bond*, Oxford University Press, Oxford, U.K., 1999.
(15) Craig, D. P.; Mellor, D. P. *Top. Curr. Chem.* **1976**, *63*, 1–48.
(16) (a) Balle, T. J.; Flygare, W. H. *Rev. Sci. Instrum.* **1981**, *52*, 33–45. (b) Andresen, U.; Dreizler, H.; Grabow, J.-U.; Stahl, W. *Rev. Sci. Instrum.* **1990**, *61*, 3694–3699.
(17) Xu, Y.; Jäger, W. *J. Chem. Phys.,* **1997**, *106*, 7968–7980.
(18) Frisch, M. J.; et al., *Gaussian 03,* revision B.01; Gaussian Inc.: Pittsburgh, PA, 2003.
(19) Binkley, J. S.; Pople, J. A. *Int. Quantum Chem.* **1975**, *9*, 229–236.
(20) Krishman, R.; Binkley, J. S.; Seeger, R.; Pople, J. A. *J. Chem. Phys.* **1980**, *72*, 650–654.
(21) Boys, S. F.; Bernardi, F. *Mol. Phys.* **1970**, *10*, 553–566.
(22) Swalen, J. D.; Herschbach, D. R. *J. Chem. Phys.* **1957**, *27*, 100–108.
(23) Herschbach, D. R.; Swalen, J. D. *J. Chem. Phys.* **1958**, *29*, 761–776.
(24) No splitting due to the methyl internal rotation of propylene oxide was detected in all the transitions observed. We therefore assume that this motion is quenched in the complex owing to the strong intermolecular interactions that elevate the internal rotation barrier.
(25) Creswell, R. A.; Schwendeman, R. H. *J. Mol. Spectrosc.* **1977**, *64*, 295–301.
(26) Imachi, M.; Kuczkowski, R. L. *J. Mol. Struct.* **1982**, *96*, 55–60.
(27) Scharge, T.; Emmeluth, C.; Häber, Th.; Suhm, M. A. *J. Mol. Struct.* **2006**, *786*, 86–95.

gauche, and trans types. The compact gauche conformers $G-g+$ and its mirror image $G+g-$ (Figure 1 top left), were found to be dominant experimentally with electron diffraction,[28] microwave,[29] infrared,[30,31] NMR,[31] matrix isolation FTIR spectroscopy,[32–35] and microwave-infrared double resonance techniques.[36] Their dominance was also confirmed by theoretical calculations.[37–39] The greater stability of the compact gauche conformers has been commonly attributed to the stabilizing effect of an attractive intramolecular O−H···F H-bond.[28–30,37–39] However, it has also been interpreted purely as the gauche effect,[31] that is the tendency of vicinal electronegative substituents to adopt gauche conformation.[40,41] Open gauche and trans FE conformers are predicted to be at least 8 kJ mol^{-1} higher in energy (ref 27 and references therein). The relative arrangements of the PO and FE subunits can be classified as *syn* or *anti*, referring to the case where FE binds to the oxygen acceptor on the same side as the PO methyl group or on the opposite side, respectively. Together with the possibility of *syn* or *anti* arrangement, this leads to $2 \times 9 = 18$ possible conformers. If one also considers both *R* and *S* enantiomers of PO, the total number increases to $2 \times 18 = 36$ different structures. These form eighteen pairs of enantiomers. Since each such enantiomeric pair results in the same rotational spectrum and the two structures are indistinguishable in our study, we use *R*-PO throughout this work and omit this notation in the rest of the report.

Fourteen out of the eighteen proposed structures were identified as true minima in the ab initio calculations. An overview of the fourteen binary PO···FE conformers is given in the lower part of Figure 1, using a simple stick representation. The primary interaction site for all the PO···FE conformers is an O−H···O H-bond directed from FE to PO. The FE O−H donor group is indicated with an arrow, while the PO acceptor oxygen is marked with a dark circle. The position of the fluoro atom is indicated with a gray circle. The PO···FE conformers are labeled with *syn* or *anti*, followed by the conformation of the FE subunit. The FE conformation shows only small distortion upon complexation, justifying the use of the nomenclature. On the basis of the FE monomer conformation, we also group the PO···FE conformers into compact gauche, open gauche, and trans types, as shown in Figure 1. The calculated rotational constants and electric dipole moment components of the *anti* and *syn* PO···FE conformers, obtained in the geometry optimizations, are summarized in Tables 1 and 2, respectively, together with the relevant torsional angles of the FE subunit and the corresponding dissociation energies. The structural relevant angles and dihedral angles, as well as the geometries, of the fourteen PO···FE conformers are given in Table S1 and Figure S1, available as Supporting Information.

4. Assignment of the Rotational Spectra. From Tables 1 and 2, one can see that the four most stable conformers were all predicted to have dominantly *b*-type transitions whose patterns are generally more difficult to recognize than *a*-type transitions.

Table 1. Rotational Constants, Electric Dipole Moment Components, Relevant Torsional Angles, and Raw (D_e) and ZPE-Corrected (D_0) Dissociation Energies Are Given for the Seven *Anti* PO···FE Conformers, Calculated at the MP2/6-311++G** Level of Theory[a]

	anti						
conformer	compact gauche		open gauche		trans		
	G−g+	*G+g−*	*G+g+*	*G−g−*	*Tg+*	*Tg−*	*Tt*
A (MHz)	3312	3230	3708	2729	3332	3734	6771
B (MHz)	942	945	870	1193	667	632	493
C (MHz)	849	858	771	920	622	592	484
$\lvert\mu_a\rvert$ (D)	0.4	0.7	1.3	1.7	5.3	5.2	4.8
$\lvert\mu_b\rvert$ (D)	2.7	2.7	0.9	0.6	0.1	0.2	0.3
$\lvert\mu_c\rvert$ (D)	0.5	1.0	1.3	1.3	0.4	0.2	1.1
$\tau_{O-C-C-F}$ (°)	−67.8	67.8	62.6	−62.1	179.5	−179.4	−177.5
$\tau_{H-O-C-C}$ (°)	73.1	−73.0	48.6	−45.3	65.7	−66.1	−169.4
D_e (kJ mol^{-1})	34.95	34.79	28.25	29.64	24.98	24.89	24.05
	[23.56]	[23.37]	[18.02]	[18.10]	[15.82]	[15.77]	[15.22]
D_0 (kJmol^{-1})	30.06	29.94	23.16	24.56	20.12	20.14	20.03
	[18.67]	[18.51]	[12.93]	[13.02]	[10.96]	[11.02]	[11.21]

[a] BSSE corrected values are given in parentheses.

Table 2. Rotational Constants, Electric Dipole Moment Components, Relevant Torsional Angles, and Raw (D_e) and ZPE-Corrected (D_0) Dissociation Energies Are Given for the Seven *Syn* PO···FE Conformers, Calculated at the MP2/6-311++G** Level of Theory[a]

	syn						
conformer	compact gauche		open gauche		trans		
	G−g+	*G+g−*	*G+g+*	*G−g−*	*Tg+*	*Tg−*	*Tt*
A (MHz)	2734	2796	2812	2986	3707	3174	5143
B (MHz)	1067	1064	1061	1027	680	752	565
C (MHz)	988	985	936	898	648	748	531
$\lvert\mu_a\rvert$ (D)	0.9	0.5	2.5	1.2	5.0	4.9	4.9
$\lvert\mu_b\rvert$ (D)	2.8	2.1	0.3	1.4	0.5	0.0	0.2
$\lvert\mu_c\rvert$ (D)	0.9	0.8	2.1	1.2	0.1	0.7	0.6
$\tau_{O-C-C-F}$ (°)	−68.7	67.4	62.9	−62.2	179.4	179.8	175.9
$\tau_{H-O-C-C}$ (°)	71.6	−78.4	50.1	−48.7	65.2	−65.9	160.4
D_e (kJmol^{-1})	33.53	34.91	28.77	28.97	25.79	26.05	24.72
	[22.22]	[23.36]	[17.39]	[18.32]	[16.38]	[16.14]	[15.90]
D_0 (kJmol^{-1})	28.46	29.98	23.63	23.71	20.74	21.17	20.26
	[17.15]	[18.43]	[12.25]	[13.06]	[11.32]	[11.27]	[11.44]

[a] BSSE corrected values are given in parentheses.

Extensive frequency scans and sample testing were therefore performed. The initial search scans were carried out in the 4 to 8.3 GHz frequency region, using a microwave pulse length of 1.0 μs, optimized empirically for molecules with a dipole moment of 2∼3 Debye. Lines due to the previously investigated species PO monomer,[22,23,25] FE monomer,[28,36] PO···Ne,[42,43] and PO dimer[44] could be easily recognized and eliminated from the data set of candidates for the PO···FE transitions. The remaining lines were further tested in a FE/PO/Ne sample to discard any transitions due to Ne containing species. In addition, lines appearing in a FE/Ne sample were also removed from the list for PO···FE. The remaining transitions observed were then used in the initial assignments, with the aid of the calculated rotational constants listed in Tables 1 and 2. Three low *J b*-type transitions, for example, $1_{11}-0_{00}$, $2_{12}-1_{01}$, $3_{13}-2_{02}$ or $4_{04}-3_{13}$, were assigned first. More corresponding *a*-, *b*-, and *c*-type transitions were then measured or identified from the list of transitions observed. In this manner, three PO···FE conformers could be assigned. An example survey scan in the frequency region of 5–6 GHz, recorded with a step size of 0.2 MHz, with trace amounts of PO and FE in Ne, is shown in Figure 2.

(28) Huang, J.; Hedberg, K. *J. Am. Chem. Soc.* **1989**, *111*, 6909–6913.
(29) Buckton, K.; Azrak, R. G. *J. Chem. Phys.* **1970**, *52* (11), 5652–5655.
(30) Buckley, P.; Giguère, P. A.; Yamamoto, D. *Can. J. Chem.* **1968**, *46*, 2917–2923.
(31) Bakke, J. M.; Bjerkeseth, L. H.; Rønnow, T. E. C. L.; Steinsvoll, K. *J. Mol. Struct.* **1994**, *321*, 205–214.
(32) Gounev, T. K.; Bell, S.; Zhou, L.; Durig, J. R. *J. Mol. Struct.,* **1998**, *447*, 21–32.
(33) Frei, H.; Pimentel, G. C. *Annu. Rev. Phys. Chem.* **1985**, *36*, 491–524.
(34) Pourcin, J.; Monnier, M.; Verlaque, P.; Davidovics, G.; Lauricella, R.; Colonna, C.; Bodot, H. *J. Mol. Spectrosc.* **1985**, *109*, 186–201.
(35) Shirk, J. S.; Marquardt, C. L. *J. Chem. Phys.,* **1990**, *92* (12), 7234–7240.
(36) Green, D.; Hammond, S.; Keske, J.; Pate, B. H. *J. Chem. Phys.* **1999**, *110* (4), 1979–1989.
(37) Radom, L.; Lathan, W. A.; Hehre, W. J.; Pople, J. A. *J. Am. Chem. Soc.* **1973**, *95* (3), 693–698.
(38) Dixon, D. A.; Smart, B. E. *J. Phys. Chem.* **1991**, *95*, 1609–1612.
(39) Buemi, G. *J. Chem. Soc., Faraday Trans.* **1994**, *90* (9), 1211–1215.
(40) Wolfe, S. *Acc. Chem. Res.* **1972**, *5*, 102–111.
(41) Freitas, M. P.; Rittner, R. *J. Phys. Chem. A* **2007**, *111*, 7233–7236.
(42) Blanco, S.; Maris, A.; Melandri, S.; Caminati, W. *Mol. Phys.* **2002**, *100*, 3245–3249.
(43) Su, Z.; Xu, Y. *J. Mol. Spectrosc.* **2005**, *232*, 112–114.
(44) Su, Z.; Borho, N.; Xu, Y. *J. Am. Chem. Soc.* **2006**, *128*, 17126–17131.

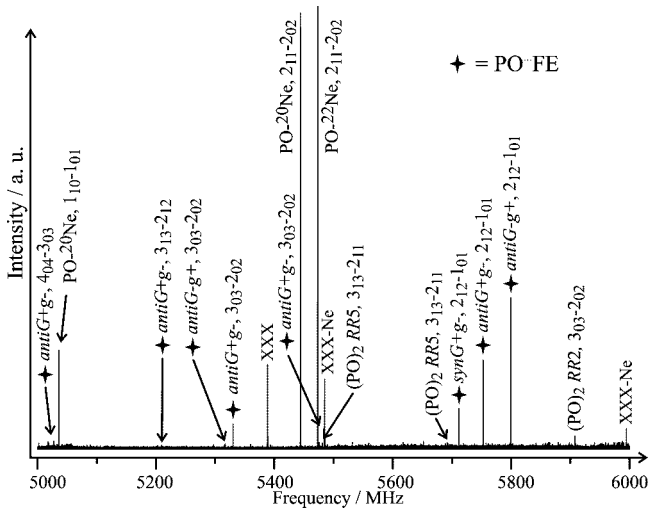

Figure 2. An example survey scan with a sample mixture consisting of 0.3% FE and 0.3% PO in Ne at 2–4 bar.

Table 3. Experimental Rotational and Centrifugal Distortion Constants of the Three PO···FE Conformers

	conformer 1 (*anti G−g+*)	conformer 2 (*anti G+g−*)	conformer 3 (*syn G+g−*)
A (MHz)	3273.490(1)	3218.821(1)	2785.1628(3)[a]
B (MHz)	933.8656(3)	935.5612(2)	1049.8488(2)
C (MHz)	842.0002(2)	844.6205(2)	975.4717(2)
D_J (kHz)	0.442(5)	0.436(3)	0.615(4)
D_{JK} (kHz)	1.31(2)	−0.31(1)	2.44(1)
D_K (kHz)	4.3(3)	8.2(3)	−1.77(3)
D_1 (kHz)	−0.0194(8)	−0.008(1)	−0.051(2)
D_2 (kHz)	0.0136(3)	0.0129(2)	0.0294(7)
κ	−0.9244	−0.9234	−0.9178
N[b]	43	58	39
σ[c] (kHz)	1.6	4.4	1.8

[a] Standard error in parentheses are expressed in units of the last digits. [b] Number of transitions in the fit. [c] Root-mean-square deviation of the fit.

Lines labeled with xxx···Ne or xxx in Figure 2 may originate from PO···FE···Ne$_x$ or PO$_x$···FE$_x$ complexes, but are not yet assigned. The assigned transitions of PO···Ne, PO dimer and PO···FE are labeled accordingly. The spectroscopic constants obtained from the fits to a semirigid rotor Hamiltonian using Watson *S*-reduction and I^r representation are summarized in Table 3. In total, 43, 58, and 39 lines, including all *a-*, *b-*, and *c*-type transitions, were measured for the three conformers 1, 2, and 3, respectively. The measured transitions and their assignments are given in Tables S2−S4, available as Supporting Information.

The rotational constants of the compact gauche, open gauche, and trans PO···FE conformers differ significantly, and it is apparent from a comparison of the experimental rotational constants in Table 3 with the predictions in Tables 1 and 2, that all three observed conformers belong to the compact gauche group. The structures of the four PO···FE conformers of the compact gauche group, *anti G−g+*, *anti G+g−*, *syn G−g+* and *syn G+g−* are visualized in Figure 3. Each of them exhibits a delicate H-bond network, with an intermolecular O−H···O, an intramolecular O−H···F, and two intermolecular C−H···F connections. The shapes and therefore the rotational constants of the two *syn* conformers are significantly different from the two *anti* ones. This makes it relatively straightforward to identify that the experimentally observed conformer 3 belongs to the *syn* group and that conformers 1 and 2 belong to the *anti* group. The root-mean-square of the experimental minus calculated rotational constants is smaller for the assignment of conformer 3 to *syn G+g−* (44 MHz) than to *syn G−g+* (105 MHz). The differences in the experimental rotational constants *A*, *B*, and *C* of conformers 1 and 2 are 54.7, −1.7, and −2.6 MHz, respectively, while the corresponding differences in the calculated rotational constants of conformers *anti G−g+* and *anti G+g−* are 82, −3, and −9 MHz. We therefore assigned 1 → *anti G−g+* and 2 → *anti G+g−*. Though the assignment here is based on the frequency information, additional support for the assignment comes from the detailed comparison of the trends of the observed and calculated dipole moment components. Longer optimized excitation pulse lengths were observed experimentally for the *a-* and *c*-type transitions of *anti G−g+* as compared to *anti G+g−*. This is in agreement with the prediction that the μ_a and μ_c dipole moment components of *anti G−g+* (0.4 and 0.5 D, respectively) are smaller than those of *anti G+g−* (0.7 and 1.0 D, respectively). Very similar *b*-type transition intensities were detected experimentally for the two *anti* conformers whose *b*-dipole moments were both predicted to be 2.7 Debye. This suggests an almost equal abundance in the expansion and therefore similar dissociation energies for the two *anti* conformers. The experimental *b*-type transition intensities for the *syn* conformer, on the other hand, are significantly weaker. All these point to an energy ordering of *anti G−g+* ≈ *anti G+g−* < *syn G+g−*, experimentally.

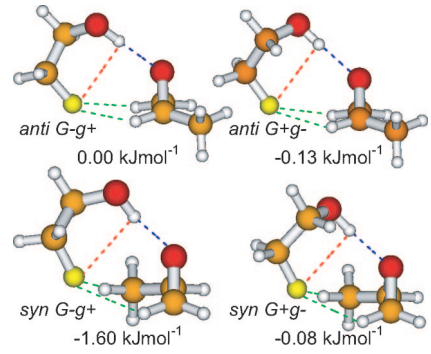

Figure 3. Structures of the four compact gauche PO···FE conformers, as predicted by MP2/6-311++G** calculations. The relative dissociation energies ΔD_0 with respect to the *anti G−g+* conformer are also indicated.

About 20 unassigned rotational transitions in the scans were identified as originating from the PO···FE complexes. Several attempts to assign them to *syn G−g+*, the fourth most stable conformer predicted, or to the other remaining conformers were not successful. The $2_{12}-1_{01}$ transitions of the three observed conformers all fall in the small range between 5.7 and 5.8 GHz, and all have been detected in the survey scan displayed in Figure 2. If the fourth conformer were of similar abundance in the jet expansion, the $2_{12}-1_{01}$ *b*-type transition of the *syn G−g+* conformer with a comparable *b*-dipole moment component and similar rotational constants should have been detected. We therefore conclude that only three PO···FE conformers are formed selectively in the PO/FE/Ne coexpansion.

5. Results and Discussion

5.1. Stability Ordering of the PO···FE Conformers. To understand the selective formation of the 3 out of 14 PO···FE conformers in the jet expansion, we examine the predicted dissociation energies D_0 that are summarized in Tables 1 and 2. Figure 4 visualizes the energy ordering of the 14 PO···FE conformers by displaying the relative dissociation energies ΔD_0, with respect to the most stable conformer *anti G−g+*. The relative energy ordering of the corresponding FE monomers is also included in Figure 4. The direct comparison of the relative energies of free FE and PO···FE reveals that the strong preference of the compact gauche conformers is already present among the FE monomer conformers. The difference in the FE monomer energies is the primary contributor to the PO···FE

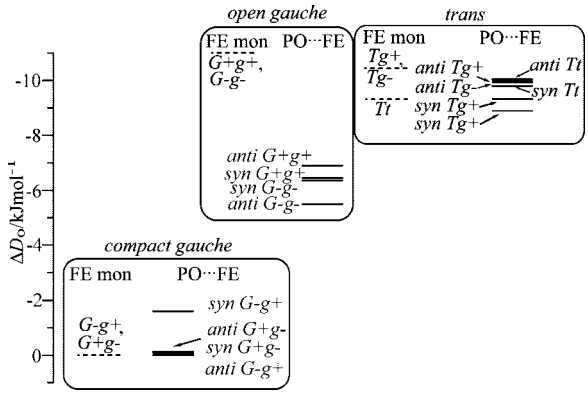

Figure 4. Energy diagram of the PO···FE conformers showing the dissociation energies ΔD_0 relative to the most stable *anti* $G-g+$ conformer. The relative FE monomer energies with respect to the compact gauche FE monomer are marked with dotted lines.

energy ordering. The calculated intermolecular interaction energy[45,46] (Table S2) of PO···FE is larger for the open gauche conformers than for the compact gauche conformers, and is the smallest for the trans conformers. As a result, the open gauche PO···FE structures are stabilized more compared to the compact gauche and trans conformers upon complexation with PO. The intermolecular interaction energy is the second most important contribution to the PO···FE energy ordering. A detailed analysis of the energy ordering, including the intermolecular interaction, and the monomer deformation energies, as well as the effects of ZPE and BSSE corrections, is given in Table S2, available as Supporting Information. Overall, the four compact gauche conformers are predicted to be more stable than the ten open gauche and trans conformers by more than 6 kJmol^{-1}. The open gauche and trans conformers will therefore have no appreciable population in a jet expansion with a typical rotational temperature of 5 K and a conformational temperature of 60 K for H-bonded complexes.[47] This prediction is consistent with the experimental observation that only conformers belonging to the compact gauche group were detected.

In these binary conformers, FE, which has two flexible bonds, does not change its monomer conformation dramatically upon complexation. Therefore, we interpret the current system as a case of a rigid lock-and-key[2] interaction rather than an example of the induced fit theory.[7] A remarkable example for the latter case is the tryptamine−water complex, which has been the subject of many experimental studies, including the methods of rotational coherence spectroscopy,[48] resonant two-photon ionization and resonant ion-dip IR spectroscopy,[49] and high resolution laser induced fluorescence spectroscopy.[50] The tryptamine−water interaction was reported to show strong structural selectivity by locking tryptamine into one high energy conformation out of the possible 27.[51]

Table 4. Analysis of the Chirality-Dependent Energy Discrimination in the PO··· FE Complex

diastereomers	raw[a]	+ZPE[a]	+ZPE+BSSE[a]	sign (exp.)
ΔE_{chi} (Diastereomeric) (kJ mol^{-1})				
(*anti* $G+g-$) − (*anti* $G-g+$)	−0.16	−0.12	−0.16	∼0
(*syn* $G+g-$) − (*syn* $G-g+$)	1.38	1.52	1.28	+[b]
ΔE_{chi} (Diastereofacial) (kJ mol^{-1})				
(*syn* $G+g-$) − (*anti* $G+g-$)	0.12	0.04	−0.08	−
(*syn* $G-g+$) − (*anti* $G-g+$)	−1.42	−1.60	−1.52	−[b]

[a] Derived from raw (D_e), ZPE corrected (D_0), and both ZPE and BSSE corrected dissociation energy values as given in Tables 1 and 2. [b] The *syn* $G-g+$ conformer was not observed experimentally and it was concluded that it has the smallest dissociation energy out of the four conformers under consideration. See text for details.

5.2. Chirality-Dependent Energy Discrimination. In the following, we will discuss the subtle energy differences among the compact gauche conformers in terms of the chiral discrimination forces at play. Chiral molecules with *R*- or *S*-configuration can form homochiral (*RR* or *SS*) or heterochiral (*RS* or *SR*) dimers. These dimers are diastereomers to each other and differ in their binding energies. This energy difference is usually referred to as *chirodiastaltic* energy ΔE_{chi}.[15,52] The PO···FE dimer exhibits four elements of chirality. PO has one stereocenter. A second stereocenter is created at the acceptor oxygen via H-bonding. In addition, two elements of helical chirality are present in FE. The gauche+ (+60°) arrangement of the two torsional angles $\tau_{O-C-C-F}$ and $\tau_{H-O-C-C}$ can be interpreted as a positive helix (equivalent to *R*-configuration), and gauche- (−60°) as a negative helix (*S*-configuration). We define the pairs of diastereomers following the notation of Portmann et al., and in a similar way as for PO···ethanol,[9] and dimethyloxirane···ethanol.[47] Two types of chirality-dependent interactions, that is, diastereofacial and diastereomeric interactions, are present. Diastereofacial interaction energy is defined as the energy difference between a *syn* and an *anti* structure with similar configurations of the PO and FE subunits, for example, between *syn* $G+g-$ and *anti* $G+g-$. The diastereomeric interaction energy describes the energy difference between the binary conformers that have both *syn* or *anti* arrangement but their FE subunits are mirror images to each other, for example, *anti* $G+g-$ and *anti* $G-g+$. The values of ΔE_{chi} (diastereomeric) and ΔE_{chi} (diastereofacial), calculated from the raw (D_e), the ZPE corrected (D_0), and both ZPE and BSSE corrected (D_0+BSSE) dissociation energies, are collected in Table 4. The signs of the chirodiastaltic energies extracted from the experiments are also given in Table 4. The chiral discrimination is very subtle for the diastereomeric pair *anti* $G-g+$ and *anti* $G+g-$. The small calculated ΔE_{chi}(diastereomeric) value of −0.12 kJ mol^{-1} agrees with the similar abundance of *anti* $G-g+$ over *anti* $G+g-$ observed in the experiment. Interestingly, the chiral discrimination is significantly larger for the *syn* pair. The strong preference of *syn* $G+g-$ over *syn* $G-g+$ observed experimentally is reflected in the calculated value of 1.5 kJ mol^{-1} for ΔE_{chi} (diastereomeric). The observed preference of *anti* $G+g-$ over *syn* $G+g-$, on the other hand, is not predicted consistently, suggesting some deficiencies of the MP2 calculations in describing the subtle discrimination interactions.

5.3. Effect of Fluorination of Ethanol on Structures and Dissociation Energies. Fluorination increases the energy span among the PO···FE conformers in comparison to the

(45) Szalewicz, K.; Jeziorski, B. *J. Chem. Phys.* **1998**, *109* (3), 1198–1200.
(46) Xantheas, S. *J. Chem. Phys.* **1996**, *104*, 8821–8824.
(47) Borho, N.; Xu, Y. *Phys. Chem. Chem. Phys.* **2007**, *9*, 4514–4520.
(48) Connell, L. L.; Corcoran, T. C.; Joireman, P. W.; Felker, P. M. *J. Phys. Chem.* **1990**, *94*, 1229–1232.
(49) Carney, J. R.; Dian, B. C.; Florio, G. M.; Zwier, T. S. *J. Am. Chem. Soc.* **2001**, *123*, 5596–5597.
(50) Schmitt, M.; Böhm, M.; Ratzer, C.; Vu, C.; Kalkman, I.; Meerts, W. L. *J. Am. Chem. Soc.* **2005**, *127*, 10356–10364.
(51) (a) Nguyen, T. V.; Pratt, D. W. *J. Chem. Phys.* **2006**, *124*, 054317-1–054317-6. (b) Nguyen, T. V.; Korter, T. M.; Pratt, D. W. *Mol. Phys.* **2005**, *103*, 1603–1613.
(52) Portmann, S.; Inauen, A.; Lüthi, H. P.; Leutwyler, S. *J. Chem. Phys.* **2000**, *113*, 9577–9585.

PO···ethanol conformers by more than an order of magnitude, from ~0.7 kJ mol^{-1} for the six conformers of PO···ethanol to ~10.0 kJ mol^{-1} for the fourteen PO···FE conformers. The effect is due mainly to the significantly larger energy differences among the FE conformers than among the ethanol conformers, which are transferred to the corresponding binary systems. In addition, the extra functional group introduced by monofluorination also provides more contact points and stronger intermolecular interactions. A major difference between PO···FE and PO···ethanol is the orientation of the H-bond donor subunit, that is, FE or ethanol, with respect to PO. In PO···ethanol, the aliphatic part of ethanol points away from the oxirane ring. In contrast, the CH_2F-CH_2- chain of FE turns toward the PO molecule in PO···FE (see Figure 3). This arrangement allows for the formation of C−H···F interactions that are absent in the PO···ethanol conformers. An overview of the intra and intermolecular H-bonding network in the PO···FE complex is given in Table S6, available as Supporting Information. All conformers of the compact gauche group exhibit two short C−H···F distances, while members of the open gauche group show one short or two long C−H···F distances, and conformers of the trans group have no close C−H···F contacts. The number of the secondary interactions correlates with the calculated energy ordering. On the whole, the PO···FE conformers involving the most stable compact gauche arrangement gain stability of about 5 kJ mol^{-1} with respect to the PO···ethanol conformers, while the other arrangements exhibit destabilization of up to 5 kJ mol^{-1}. As a result, all six PO···ethanol conformers were detected experimentally, while only three out of the fourteen PO···FE conformers were observed under similar experimental conditions. This observation is a manifestation of strongly enhanced molecular recognition upon fluorination.

Upon fluorination, chiral recognition stays subtle for the *anti* diastereomeric pair, but is enhanced for the pair *syn* $G-g+$ and *syn* $G+g-$. The diastereofacial energy discrimination changes sign upon fluorination, since PO···FE favors *anti* structures, whereas PO···ethanol prefers *syn* arrangements. This can be largely attributed to the fact that the *anti* PO···FE structures can establish optimum C−H···F interactions, whereas the *syn* PO···ethanol geometries profit from dispersive interactions of the PO methyl group and the aliphatic ethanol group. We conclude from the larger energy discrimination among the PO···FE conformers and from the enhancement of chiral recognition for the *syn* pair, that fluorination brings a higher specificity to the intermolecular interaction. Therefore, we classify FE as a "tailored" key to the PO lock, in the picture of a microscopic lock-and-key model system. This is in contrast to the recent report by Giardini et al., who found a reduced enantioselectivity for 1-phenyl-2,2,2-trifluoroethanol···2-aminobutane complexes as compared to 1-phenyl-ethanol···2-aminobutane complexes via resonant two-photon ionization spectroscopy.[53]

(53) Giardini, A.; Cattenacci, G.; Paladini, A.; Piccirillo, S.; Satta, M.; Rondino, F.; Speranza, M. *J. Phys. Chem. A* **2007**, *111*, 12559–12563.

6. Conclusion

The conformational isomerism of the PO···FE complex has been investigated in detail using quantum mechanical calculations and jet-cooled rotational spectroscopy. Fourteen PO···FE conformers were predicted theoretically. The rotational transitions of two *anti* and one *syn* conformers were observed and assigned. In all three conformers, the FE subunit remains in its favorable compact gauche, that is, $G-g+$ and $G+g-$, conformation. The experimental stability trend is *anti* $G-g+ \approx$ *anti* $G+g- <$ *syn* $G+g-$. This ordering is not reproduced consistently with the MP2/6-311++G** calculations. Fluorination introduces a dramatic increase of more than an order of magnitude in the discrimination energy for the PO···FE conformers compared to the PO···ethanol conformers. This is attributed to the ability of 2-fluoroethanol to form directional intramolecular O−H···F and intermolecular C−H···F bonds. Referring to Fischer's lock-and-key metaphor, this is tantamount to an increase of the number of contact points between lock and key via tailoring the key component. In the PO···FE complex, FE does not rearrange upon complexation, despite its two flexible bonds, and this is an example of a rigid lock-and-key interaction and not of the induced fit theory. This study is one example of applying high resolution spectroscopy, in combination with ab initio calculations, to obtain conformational resolved, accurate molecule structural information of ligand–receptor model systems.

Acknowledgment. This research was funded by the University of Alberta, the Natural Sciences and Engineering Research Council of Canada, the Canada Foundation for Innovation (New Opportunity), and Alberta Ingenuity (New Faculty Award and New Faculty Extension Award). We thank W. Jäger for the instrument time on the microwave spectrometer, R. Lehnig, J. Park, and Z. Su for discussions and their assistance, and X. Liu for comments on the manuscript. We are grateful to T. Scharge, C. Emmeluth, Th. Häber, and M. A. Suhm for kindly providing detailed information on their investigation of the FE dimers. N.B. thanks Alberta Ingenuity and the German Academic Exchange Service (DAAD) for postdoctoral fellowships.

Supporting Information Available: Complete ref 18. Summary of the important intermolecular structural parameters for all fourteen conformers of the PO···FE complex; atom labeling for PO···FE, summary of the relative binding energies of the 14 PO···FE conformers and analysis of the contributing conformation, interaction and distortion energies, including energy term definitions and reaction scheme; summary of all the measured transition frequencies of the *anti* $G-g+$,*anti* $G+g-$, and *syn* $G+g-$ PO···FE conformers; graph of the fourteen FE structures optimized at the MP2/6-311++G** level of theory; summary of the primary and secondary hydrogen-bond distances in the PO···FE interaction pair derived from the optimized structures at the MP2/6-311++G** level of theory. This material is available free of charge via the Internet at http://pubs.acs.org.

JA0783411